Hao-wen SHU, Ming JIN, Yuan-sheng TAO, Xing-jun WANG, 2019. Graphene-based silicon modulators. *Frontiers of Information Technology & Electronic Engineering*, 20(4):458-471. https://doi.org/10.1631/FITEE.1800407

Graphene-based silicon modulators

Key words: Silicon photonics; Graphene; Optical modulator

Corresponding author: Xing-jun WANG
E-mail: xjwang@pku.edu.cn
ORCID: http://orcid.org/0000-0001-8206-2544

Motivation

1. Silicon photonics is a promising technology to address the demand for dense and integrated next-generation optical interconnections. Silicon modulator suffers from several drawbacks, including a limited bandwidth, a relatively large footprint, and high power consumption.

3. Graphene-based silicon modulator, which benefits from the excellent optical properties of the two-dimensional graphene material with its unique band structure, has significantly advanced the above critical figures of merit.

Main idea

1. We review the state-of-the-art graphene-based silicon modulators operating in various mechanisms, i.e., thermal-optical, electro-optical, and plasmonic.

2. It is shown that graphene-based silicon modulators possess the potential to have satisfactory characteristics in intra- and inter-chip connections.

Major results

1. Summary of modulation theory of electro-optical (E-O) graphene silicon modulators

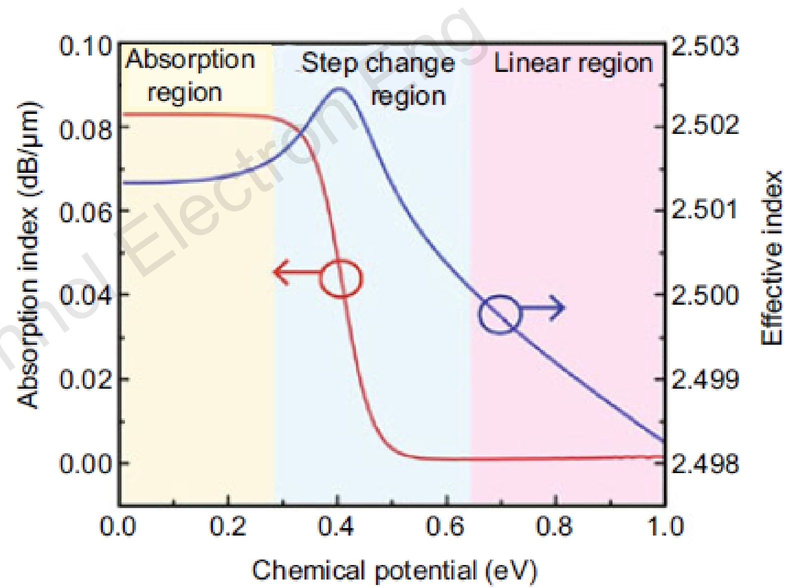

Fig. 1 Complex effective index of the graphene-oxide-silicon waveguide in 1550 nm resulting from the Kubo formula (Shu et al. (2018b), licensed under CC BY 4.0). References to color refer to the online version of this figure

Major results (Cont'd)

2. Two types of typical structure of graphene-based E-O silicon modulators

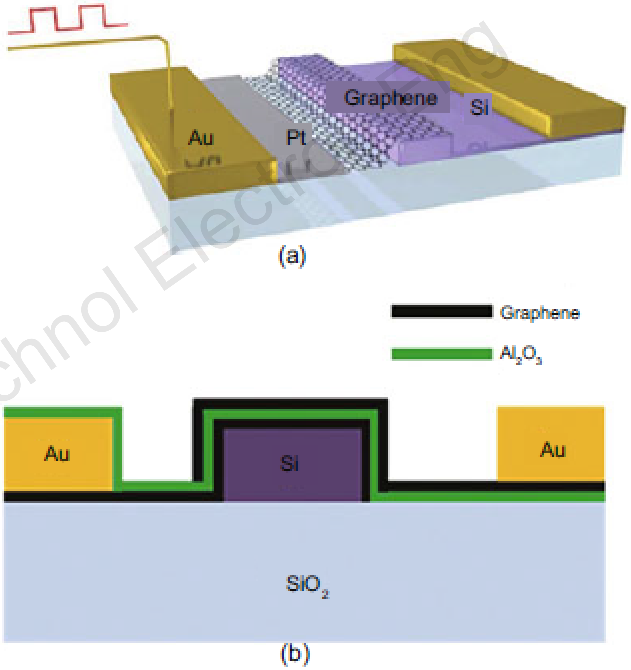

Fig. 2 Two typical structures of graphene based silicon strip waveguide modulators: (a) graphene-oxide-silicon (GOS) waveguide modulator (reprinted from Liu et al. (2011), Copyright 2011, with permission from Springer); (b) graphene-oxide-graphene (GOG) waveguide modulator (reprinted from Liu et al. (2012), Copyright 2012, with permission from American Chemical Society)

Major results (Cont'd)

3. Several optical constructions for higher performance in the graphene-based silicon modulator:

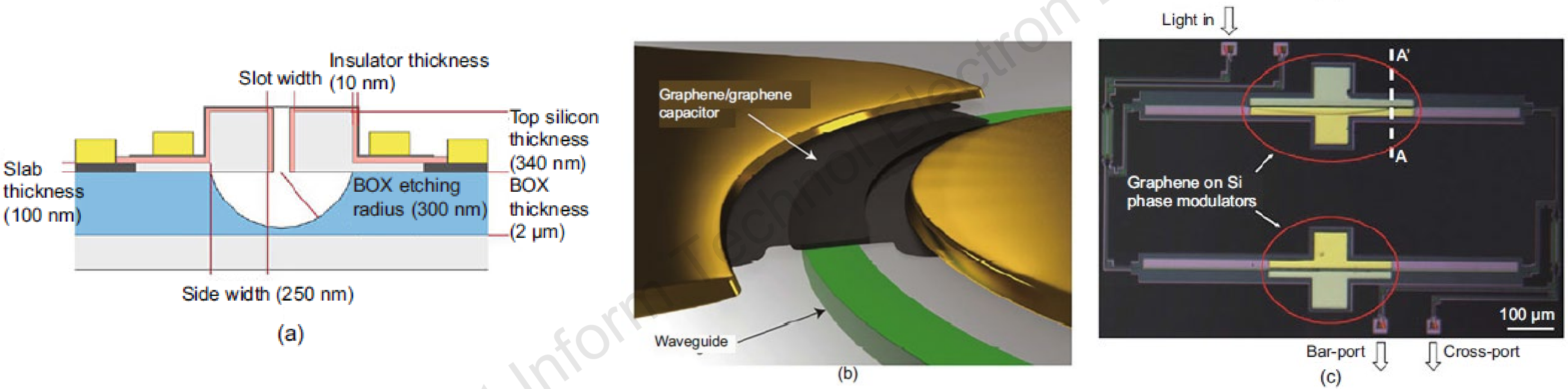

Fig. 3 Several optical constructions for higher performance in the graphene-based silicon modulator: (a) slot waveguide (reprinted from Phatak et al. (2016), Copyright 2016, with permission from The Optical Society); (b) microring (reprinted from Phare et al. (2015), Copyright 2015, with permission from Springer); (c) Mach-Zehnder interferometer (reprinted from Sorianello et al. (2018), Copyright 2017, with permission from Springer)

Major results (Cont'd)

4. Structure schematic of the graphene-silicon intensity modulator

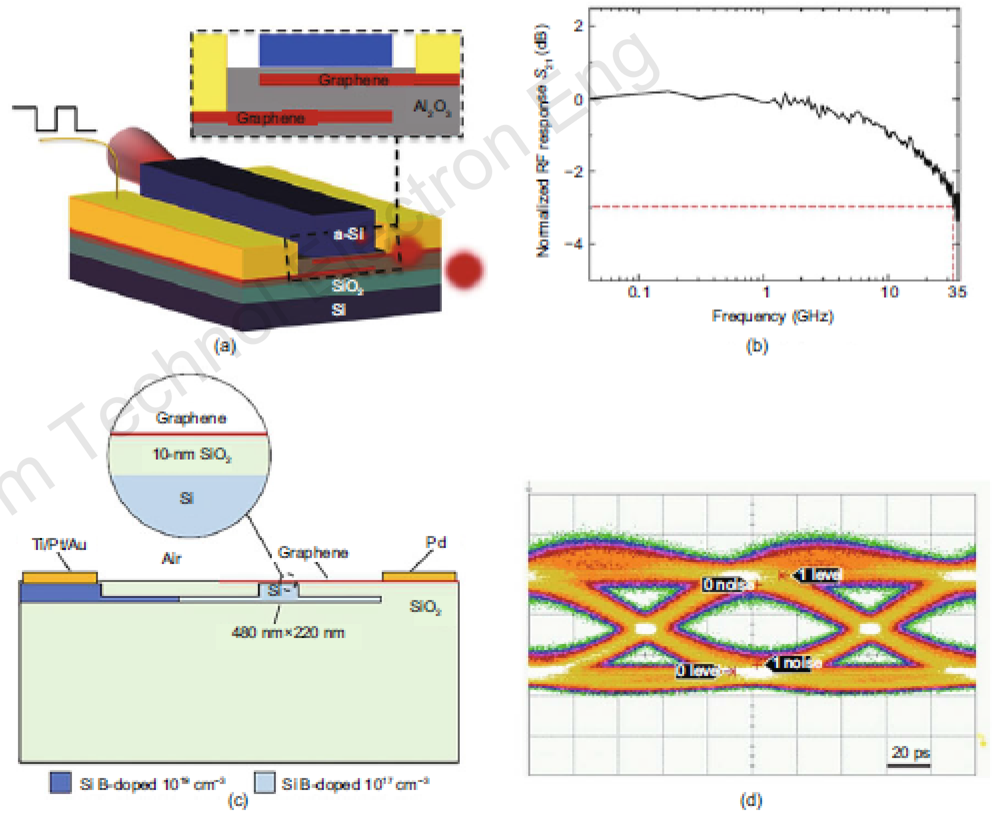

Fig. 4 Structure schematic of the graphene-silicon intensity modulator (a) (reprinted from Dalir et al. (2016), Copyright 2016, with permission from American Chemical Society), bandwidth of the absorption modulator (b) (reprinted from Dalir et al. (2016), Copyright 2016, with permission from American Chemical Society), cross-section illustration of the graphene-silicon phase modulator (c) (reprinted from Sorianello et al. (2018), Copyright 2017, with permission from Springer), and 10-Gb/s eye diagram of the phase modulator (d) (reprinted from Sorianello et al. (2018), Copyright 2017, with permission from Springer)

Major results (Cont'd)

5. Thermo-optical (T-O) graphene silicon modulators

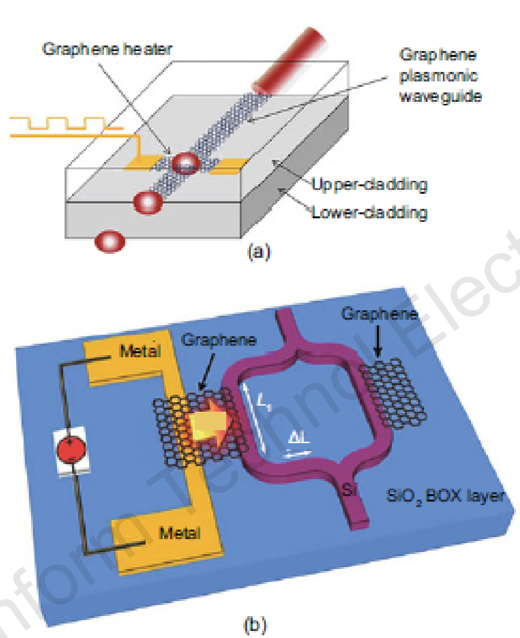

Fig. 5 Schematic view of the proposed graphene-microribbon-based thermo-optic mode: (a) the long range surface plasmonic polariton (SPP) stripe mode that propagates along the graphene stripe is extinguished (or perturbed) by thermally inducing an inhomogeneous refractive-index distribution (reprinted from Kim et al. (2013), Copyright 2013, with permission from The Optical Society); (b) 3D schematic illustration of a thermally tuning Mach-Zehnder interferometer (MZI) with a non-local traditional metal heater and a graphene-based transparent flexible heat conductor (reprinted from Yu et al. (2014), Copyright 2014, with permission from AIP Publishing)

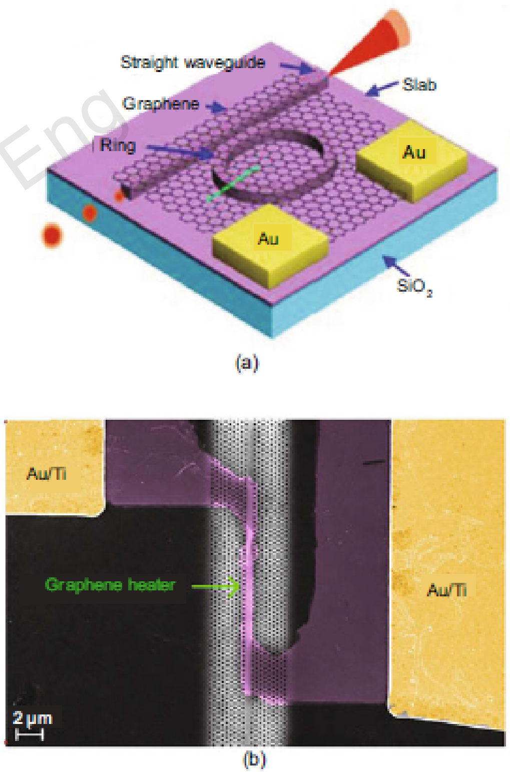

Fig. 6 Illustration of a thermo-optic microring modulator based on graphene: (a) the monolayer graphene is on top of a ring resonator without any separation layer (reprinted from Gan et al. (2015), Copyright 2015, with permission from Royal Society of Chemistry); (b) false-color scanning electron microscope image of a slow-light-enhanced graphene microheater (Yan et al. (2017), licensed under CC BY 4.0)

Major results (Cont'd)

6. All-optical graphene silicon modulators

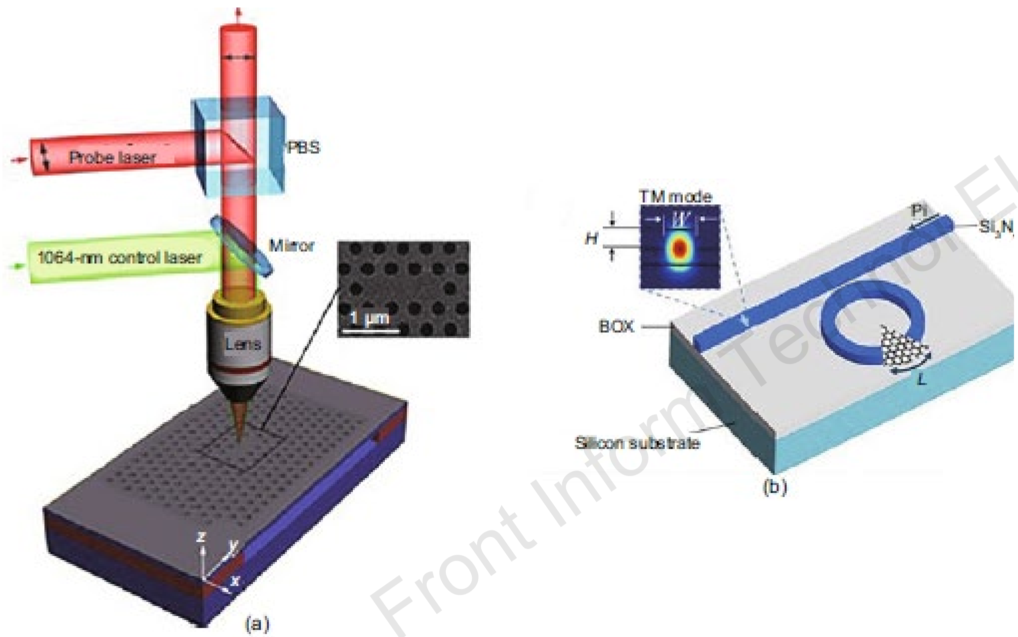

Fig. 7 Three-dimensional schematic of a graphene-cladded silicon photonic crystal cavity and the measurement setup (a) (reprinted from Shi et al. (2015), Copyright 2015, with permission from American Chemical Society) and that of a graphene-on-Si_3N_4 ring resonator device (b) (reprinted from Gao et al. (2017), Copyright 2017, with permission from The Optical Society)

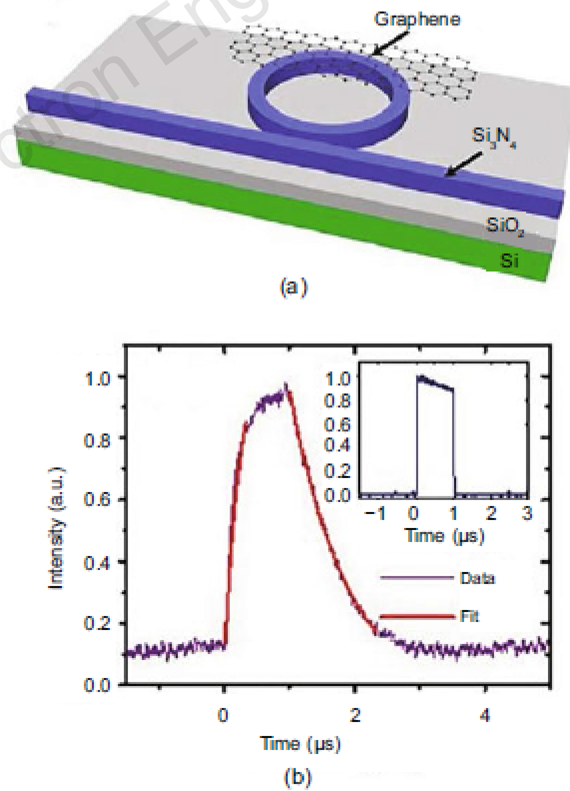

Fig. 8 Schematic of a graphene-Si_3N_4 hybrid all-optical modulator (a) and waveform of the probe output induced by a pump pulse (b) (Qiu et al. (2017), licensed under CC BY 4.0)

Major results (Cont'd)

7. Plasmonic graphene silicon modulators

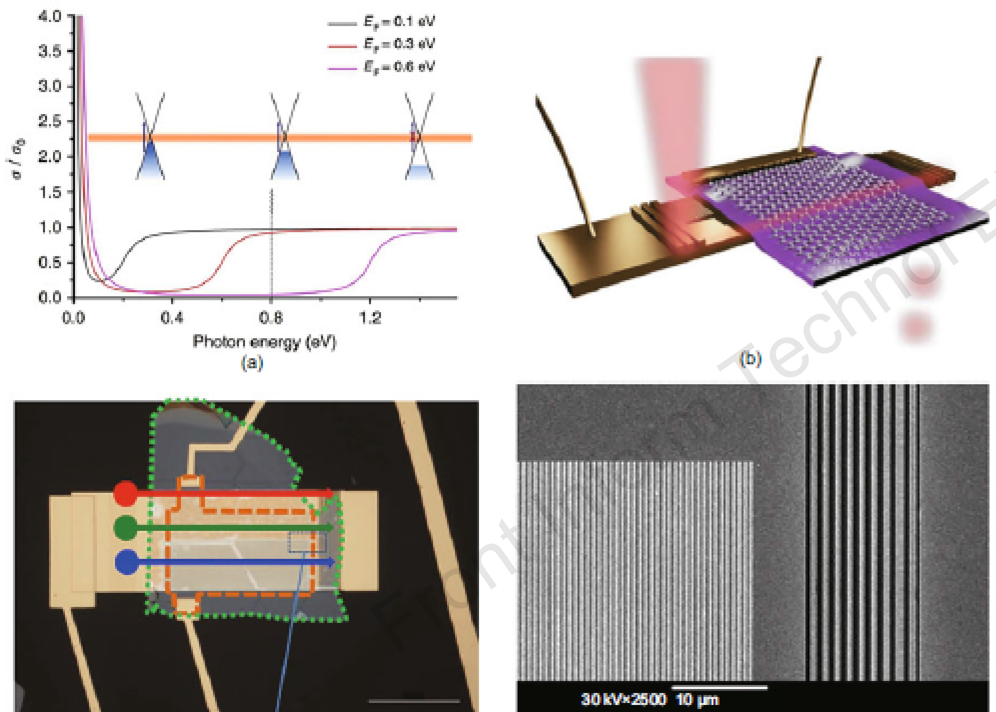

Fig. 9 Optical Pauli blocking expressed in terms of graphene relative conductivity (a), 3D rendering of the wedge plasmon mode based hybrid graphene plasmonic waveguide (b), the optical micrograph of a typical hybrid graphene plasmonic modulator studied in this work (c), and a scanning electron micrograph of an area shown in (c) by the dotted box that shows a corrugated waveguide and the semitransparent decoupling grating (d) (Ansell et al. (2015), licensed under CC BY 4.0). In (c), red, green, and blue arrows represent wedge plasmons (WP), flat plasmons (FP), and corrugated plasmons (CP) modes, respectively; the area enclosed by the green dotted line represents hBN; the area enclosed by the dotted brown line represents graphene (scale bar: 50 mm). References to color refer to the online version of this figure

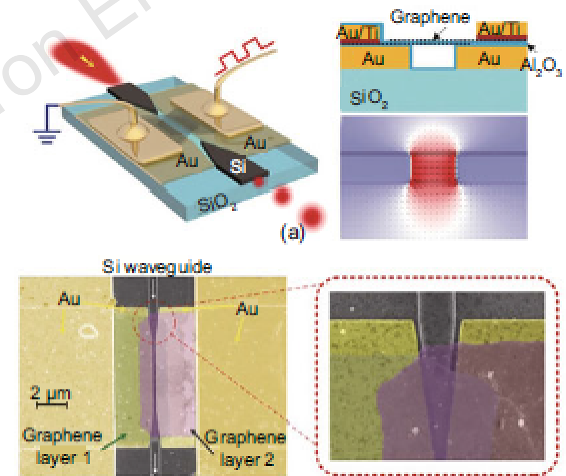

Fig. 10 Structure of the designed graphene-plasmonic hybrid slot waveguide modulator: (a) 3D schematic of the device (left), cross-section of waveguide configurations (with air being the upper cladding) (right top), and the plasmonic slot mode profile indicating how the electromagnetic field is strongly confined to the slot region (right bottom); (b) false-color SEM image of the fabricated graphene-plasmonic slot hybrid waveguide in (a) (left), and a zoom-in on the coupling part of the fabricated device (right) (reprinted from Ding et al. (2017), Copyright 2017, with permission from Royal Society of Chemistry)

Major results (Cont'd)

8. Summary of reported works

Table 1 Reported works of electro-optical (E-O), thermo-optical (T-O), all-optical, and plasmonic graphene silicon modulators

Modulator	Scheme	Size	Modulation efficiency	Year	Reference
SLG Si strip waveguide (E)	E-O (EA)	25 μm^2	0.1 dB/μm	2011	Liu et al. (2011)
DLG Si strip waveguide (E)	E-O (EA)	40 μm (length)	0.16 dB/μm	2012	Liu et al. (2012)
DLG Si_3N_4 microring (E)	E-O (EA)	40 μm (radius)	15 dB@10 V	2015	Phare et al. (2015)
DLG Si slot Mach-Zehnder (T)	E-O (ER)	100 μm (length)	0.063 V·cm	2016	Phatak et al. (2016)
SLG Si rib Mach-Zehnder (E)	E-O (ER)	300 μm (length)	0.28 V·cm	2017	Sorianello et al. (2018)
SLG Si rib Mach-Zehnder (E)	E-O (ER)	40 μm (length)	0.13 V·cm	2018	Shu et al. (2018b)
SLG Si Mach-Zehnder (E)	T-O	120 μm (length)	0.064 nm/mW	2014	Yu et al. (2014)
SLG Si microring (E)	T-O	10 μm^2	0.1 nm/mW	2015	Gan et al. (2015)
SLG Si_3N_4 microring (E)	T-O	60 μm (radius)	0.008 nm/mW	2017	Qiu et al. (2017)
SLG Si crystal cavity (E)	All-optical	—	0.06 nm/mW	2015	Shi et al. (2015)
SLG Si_3N_4 microring (E)	All-optical	—	0.023 nm/mW	2017	Gao et al. (2017)
SLG-hBN-Si waveguide (T)	Plasmonic	9 μm (length); 1.3 μm^2	21.7 dB@1.8 V	2015	Shin and Kim (2015)
SLG-hBN-SLG waveguide (T)	Plasmonic	3 μm (length)	39.75 dB@3.13 V	2016	Chen et al. (2016)
DLG slot waveguide (E)	Plasmonic	—	2.1 dB@7.5 V	2017	Ding et al. (2017)
DLG plasmonic slot waveguide (T)	Plasmonic	363 nm (length)	3 dB	2017	Hu and Wang (2017)
SLG plasmonic waveguide (E)	Plasmonic	60 nm×40 nm	2.5 dB	2018	Ono et al. (2018)

T: theoretical or simulation results; E: experimental results. SLG: single-layer graphene; DLG: double-layer graphene; hBN: hexagonal boron nitride; EA: electric-absorption modulation; ER: electric-refraction modulation

Conclusions

1. So far, graphene-based silicon modulators have made great progress at an extremely fast pace, ranging across material modulation principles, conceptual devices, fabrication processes, and primary experimental demonstrations.

2. Works including E-O graphene-silicon modulators, T-O graphene-silicon modulators, all-optical graphene-silicon modulators, and graphene-plasmonic modulators are well summarized in this work.

3. Nevertheless, there is still a significant demand for performance improvement and application practicality, which means a continuous effort to exploit effective mechanisms, practical techniques, and novel modulation configurations.